Journal of Applied Electrochemistry (2006) 36:215–226
DOI 10.1007/s10800-005-9055-1

Weight loss, polarization, electrochemical impedance spectroscopy, SEM and EDX studies of the corrosion inhibition of copper in aerated NaCl solutions

MOHAMMED A. AMIN
Chemistry Department, Faculty of Science, Ain Shams University, Abbassia, 11566, Cairo, Egypt (e-mail: maaismail@yahoo.com)

Received 14 January 2005; accepted in revised form 24 August 2005

Key words: anionic surfactant, adsorption, copper, corrosion inhibition, EIS, NaCl solution

Abstract

This work reports results of weight loss, potentiodynamic polarization and impedance measurements on the corrosion inhibition of copper in aerated non-stirred 3% NaCl solutions in the temperature range 15–65 °C using sodium oleate (SO) as an anionic surfactant inhibitor. These studies have shown that SO is a very good ''green'', mixed-type inhibitor. The inhibition process was attributed to the formation of an adsorbed film on the metal surface that protects the metal against corrosive agents. Scanning electron microscopy (SEM) and energy dispersion X-ray (EDX) observations of the electrode surface confirmed the existence of such an adsorbed film. The inhibition efficiency increases with increasing surfactant concentration and time of immersion, while it decreases with solution temperature. Maximum inhibition efficiency of the surfactant is observed at concentrations around its critical micellar concentration (CMC). The potential of zero charge (pzc) of copper was studied by ac impedance, and the mechanism of adsorption is discussed. The sigmoidal shape of the adsorption isotherm confirms the applicability of Frumkin's equation to describe the adsorption process. Thermodynamic functions for the adsorption process were determined.

1. Introduction

Copper and its alloys are applied extensively in marine environments due to their high corrosion resistance in sea water. In addition, copper dissolution in chloride solutions is very important in the electropolishing and electromachining industries. Due to these reasons attention has focused on the behaviour of copper in chloride solutions [1–6]. In the absence of different complexing agents in the corrosion medium, such as Cl^- ions, anodic dissolution of copper proceeds in two steps [7]:

$$Cu = Cu^+ + e^- \quad (1)$$

$$Cu^+ = Cu^{2+} + e^- \quad (2)$$

In neutral aqueous solutions, where oxygen is present, the overall reaction of anodic copper dissolution proceeds as follows:

$$Cu + 1/2O_2 + H_2O = Cu^{2+} + 2OH^- \quad (3)$$

When complexing agents, such as Cl^-, are present in the corrosive aqueous medium, complex copper ions, such as $CuCl_2^-$, must be considered. In the near-neutral pH range of oxygen-containing media, the anodic reactions (at least at the immersion time) are as follows [5, 6]:

$$Cu + Cl^- = CuCl_{ads} + e^-, \quad (4)$$

$$CuCl_{ads} + Cl^- = CuC1_2^- \quad (5)$$

Mass transfer effects have been shown to be significant during the anodic dissolution of copper in chloride media with cuprous chloride complexes as the major product species [8].

Even though copper corrosion in near neutral aqueous solutions is low, the damage from the corrosion products such as Cu^{2+} ions may be harmful. In most cases of copper corrosion, an additive must be added to the environment in order to modify or hinder corrosion. Azoles, specifically triazoles, have been intensively investigated as effective copper corrosion inhibitors [9–13]. Currently, research in copper corrosion is oriented to the development of ''green corrosion inhibitors'', compounds with good inhibitory efficiency but low risk of environmental pollution [14–16].

Although surfactants have been widely used, only a few studies have focused on the application of surfactants for corrosion prevention of metals and

alloys [17, 18]. In our previous study [19–21], anionic, cationic and non-ionic surfactants were successfully used as corrosion inhibitors for the acid corrosion of pure Al and some of its alloys. Under appropriate conditions, surfactant molecules may adsorb to the solid surface, forming an organized structure, i.e., the hemimicelle [17, 18], that can effectively prevent metals from corrosion in aggressive environments.

This article reports the use of weight loss, potentiodynamic polarization and impedance techniques complemented with some SEM and EDX observations to study the ability of sodium oleate (SO) as an anionic surfactant, to inhibit the corrosion of copper in aerated stagnant 3.0% NaCl solution under the influence of various experimental conditions. It was also the purpose of the present work to test the experimental data obtained from the three techniques with several adsorption isotherms at different temperatures, in order to determine the thermodynamic functions for the adsorption process and gain more information on the mode of adsorption.

2. Experimental

The working electrode employed in this work were made of spec pure copper. For weight loss measurements, corrosion inhibition tests were performed using coupons measuring $1 \times 2 \times 0.1$ cm^3 prepared from pure copper. These coupons were first briefly ground with no. 600 emery paper, subsequently polished with no. 2000 emery paper, washed with deionized water, degreased with absolute ethanol, dried, and then etched in a 7 M HNO_3 solution for 30 s. The etched electrode was rinsed with deionized water rapidly, followed by immediate rinsing with absolute ethanol. The nitric acid etching method provided a fresh and active (oxide-free) copper surface. The coupons were dried and kept in a desiccator.

The weight loss (in mg cm^{-2}) was determined at different immersion times at 25 °C by weighing the cleaned samples before and after hanging the coupon into 100 cm^3 of the corrosive solution, namely 3% NaCl, (in open air) in the absence and presence of various concentrations of SO. After the time elapsed the cleaning procedure consisted of wiping the coupons with a paper tissue and washing with distilled water and acetone, followed by oven drying at 110 °C.

For electrochemical measurements, the investigated materials were cut as cylindrical rods, welded with Cu-wire for electrical connection and mounted into glass tubes of appropriate diameter using Araldite to offer an active flat disc shaped surface of (0.20 cm^2) geometric area, to contact the test solution. Prior to each experiment, the surface pretreatment of the working electrode mentioned in weight loss measurements was performed. The experiments were performed in a 100 cm^3 volume cell at 25 °C ± 1, using Pt wire and a SCE as auxiliary and reference electrodes, respectively. The SCE was connected via a Luggin capillary, the tip of which was very close to the surface of the working electrode to minimize the IR drop. All potentials are referred to this reference electrode. The measurements were carried out in aerated non-stirred 3% NaCl solutions with and without concentrations of sodium oleate ($C_{18}H_{33}O_2^-Na^+$) as an anionic surfactant inhibitor.

The structure of the inhibitor is

$$CH_3(CH_2)_7CH{=}CH(CH_2)_7COO^-Na^+$$

The critical micellar concentration (CMC) of the surfactant was determined by plotting surface tension data against surfactant concentration at 25 °C. The value of the CMC was found to be approximately 1.50×10^{-3} M, which is in good agreement with the value obtained by Tarasova et al. [22]. All solutions were freshly prepared from analytical grade chemical reagents using doubly distilled water and were used without further purification. For each run, a freshly prepared solution as well as a cleaned set of electrodes was used. Each run was carried out in aerated stagnant solutions at the required temperature (±1 °C), using a water thermostat.

The potentiodynamic current-potential curves were carried out at a scan rate of 0.1 mV s^{-1}. Impedance measurements were carried out using AC signals of amplitude 5 mV peak to peak at the open circuit potential in the frequency range 100–0.05 Hz. A Potentiostat/Galvanostat (EG&G model 273), lock-in amplifier (model 5210) and M352 corrosion software and M398 impedance software from EG&G Princeton Applied Research were used for the polarization and impedance measurements, respectively. All impedance data were fitted to appropriate equivalent circuits using the computer program EQUIVCRT [23].

The composition and morphology of the corrosion products formed on the surface of Cu in 3% NaCl solutions in the absence and presence of 2.0×10^{-3} M SO were tested at different immersion times by EDX and SEM examinations using a Traktor TN-2000 energy dispersive spectrometer and a Joel-Jem-1200 EX II electron microscope. The Cu samples were finally washed thoroughly and submitted to 5 min of ultrasonic cleaning in order to remove loosely adsorbed ions.

3. Results and discussion

3.1. *Weight loss measurements*

Figure 1 shows the variation of the weight loss (in mg cm^{-2}) of copper with the immersion time in 3% NaCl solution in the absence and presence of various concentrations (10^{-5}–2×10^{-3} M) of SO at 25 °C. The effect of temperature (15–65 °C) on the variation of the weight loss of copper with the immersion time in (3% NaCl + 2.5×10^{-4} M SO) solution was also studied (the results obtained are not shown here). It is obvious from Figure 1 that the weight loss decreased, and therefore the corrosion inhibition strengthened, with increase in inhibitor concentration. This trend may result from the fact that adsorption and surface coverage increases with

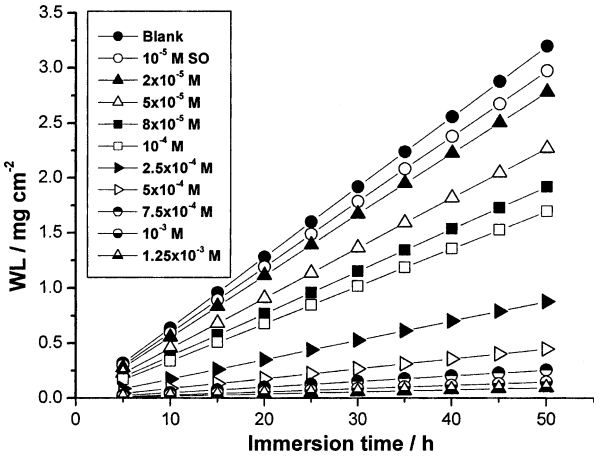

Fig. 1. Variation of the weight loss (in mg cm^{-2}) of a Cu electrode in 3% NaCl solution in the absence and presence of various concentrations of SO with the immersion time at 25 °C.

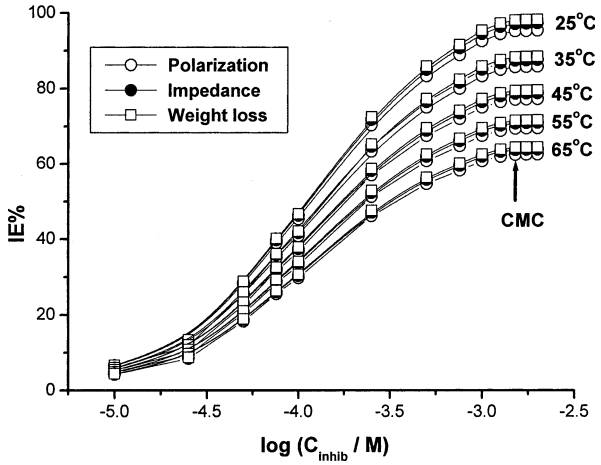

Fig. 2. Dependence of the inhibition efficiency (IE%), calculated from the weight loss, polarization and impedance data, on the logarithmic concentration of the inhibitor (log C_{inhib}) for a Cu electrode in 3% NaCl solution in the temperature range 15–65 °C.

the increase in concentration; thus the surface is efficiently separated from the medium [24].

The inhibition efficiency (IE%) (Table 1) was calculated from the total weight loss by the equation [19, 20]:

$$IE\% = [1 - (WL / WL^0)] \times 100 \quad (6)$$

where WL^0 and WL are the weight losses of specimens without and with inhibitor. Figure 2 shows plots of IE% vs. log C_{inhib} for copper at different temperatures. The plots have *S*-shaped adsorption isotherms, indicating that inhibition takes place through adsorption of the surfactant [19, 20]. At a given temperature, the inhibition efficiency increases with increasing SO concentration, and the highest inhibition efficiencies are observed when the SO concentration reaches values close to its critical micellar concentration (CMC). As the concentration of surfactant molecules approaches the CMC, micelles form in solution, and similar aggregate structures such as bilayers and multilayers form on the surface (see Figure 3). Further increase in surfactant concentration above the CMC results in other types of aggregates such as lamellar structures and rod-like micelles that can form in solution as well as analogous bilayers or multilayers that form at interfaces [17, 25].

Consequently, in the context of corrosion inhibition using surfactants, the CMC marks an effective boundary condition below which surfactant adsorption is typically below the monolayer level, and above which adsorption can consist of multiple layers of adsorbed surfactant molecules. Above the CMC, increasing surfactant concentration leads to the gradual formation of multilayers that further reduce the rate of corrosion.

Data of Figure 2 clearly show that at a given SO concentration the inhibition efficiency decreases with rise in temperature. These results may be attributed to the decrease in strength of adsorption process at higher temperatures, suggesting that physical adsorption occurs on the copper surface.

Table 1. The electrochemical parameters ($j_{corr.}$, $E_{corr.}$, b_c and b_a and R_p) associated with polarization measurements of Cu electrode in 3% NaCl solution in the absence and presence of different concentrations of the inhibitor at 25 °C

$C_{inhib.}$ × 10^5/ M	j_{corr} / mA cm^{-2}	E_{corr} / V(SCE)	b_a / V $dec.^{-1}$	b_c/ V $dec.^{-1}$	R_p / kΩ
0.0	1.080	−0.280	0.078	−0.128	1.95
1	1.010	−0.278	0.077	−0.125	2.09
2	0.940	−0.270	0.078	−0.126	2.24
5	0.780	−0.268	0.076	−0.127	2.71
8	0.660	−0.258	0.079	−0.128	3.20
10	0.590	−0.253	0.077	−0.129	3.57
25	0.320	−0.247	0.076	−0.127	6.58
50	0.180	−0.245	0.077	−0.126	11.70
75	0.120	−0.240	0.077	−0.129	17.55
100	0.080	−0.238	0.078	−0.130	26.32
125	0.060	−0.233	0.080	−0.131	35.07
150 (CMC)	0.0520	−0.228	0.078	−0.129	40.54
175	0.0510	−0.222	0.076	−0.130	41.31
200	0.050	−0.221	0.079	−0.128	42.12

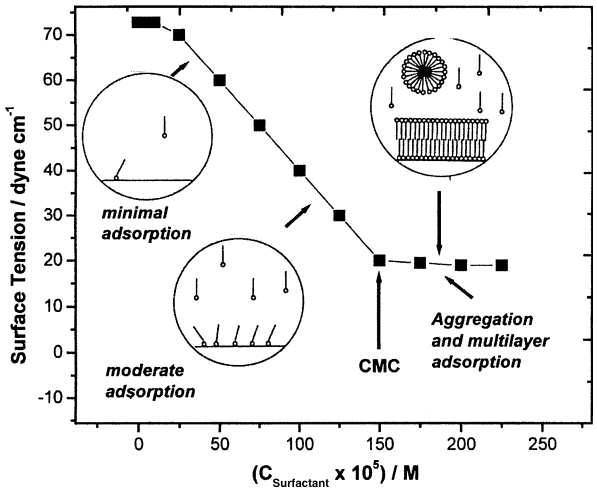

Fig. 3. Variation of the surface tension with the concentration of the inhibitor for a Cu electrode in 3% NaCl solution at 25 °C.

3.2. *Polarization measurements*

3.2.1. *Effect of inhibitor concentration*

The effect of SO concentration (10^{-5} – 2×10^{-3} M) on the anodic and cathodic polarization curves of copper in 3% NaCl solution was studied at a scan rate of 0.1 mV s^{-1} and 25 °C; some results are shown in Figure 4. For the electrode without inhibitor (curve 1), a linear relation was observed between potential and log (j) in the active dissolution region. Bacarella and Griess [1] analyzed the apparent Tafel behaviour and concluded that dissolution is controlled by the diffusion of soluble $CuCl_2^-$ species from the outer Helmholtz plane to the bulk solution. This analysis was confirmed in more detailed studies by Lee and Nobe [8]. By comparing polarization curves in the absence (curve 1) and presence of various concentrations of SO (curves 2–7) it is observed that increase in SO concentration shifts the corrosion potential (E_{corr}) in the positive direction and reduces both the anodic and cathodic current densities. These results reveal that the presence of SO in NaCl solution inhibits both the anodic and cathodic processes (mixed inhibitor). The action of SO may be related to adsorption and formation of a barrier film on the copper surface. The formation of such a barrier film is confirmed by EDX and SEM examinations of the electrode surface (see section 3.6).

The electrochemical parameters (j_{corr}, E_{corr}, b_a and b_c and R_p) associated with polarization measurements for copper at different SO concentrations were simultaneously determined from the polarization curves in the potential range (E_{corr} ± 20 mV) using M352 corrosion software from EG&G Princeton Applied Research and are listed in Table 1. The slopes of the anodic (b_a) and cathodic (b_c) Tafel lines remain almost unchanged upon addition of inhibitor. Thus the adsorbed inhibitor acts by simple blocking of active sites for both anodic and cathodic processes. In other words, the inhibitor decreases the surface area for corrosion without affecting the corrosion mechanism of copper in NaCl solutions, and only causes inactivation of a part of the surface with respect to the corrosive medium [19–21].

3.2.2. *Effect of temperature*

The influence of solution temperature (15–65 °C) on the anodic and cathodic polarization characteristics of copper in 3% NaCl solution containing (2.5×10^{-4} M SO) was studied; the results are depicted in Figure 5. Increase in solution temperature slightly shifts E_{corr} in the negative direction and enhances both the anodic and cathodic current densities. Table 2 presents the electrochemical parameters associated with polarization measurements for copper in (3% NaCl $+2.5 \times 10^{-4}$ M SO) solution at different temperatures. The j_{corr} values were used to calculate IE% of SO at different concentrations and temperatures (see Figure 2), using the equation [21].

$$IE\% = 100 \times [(j^0_{corr} - j_{corr})/j^0_{corr}] \quad (7)$$

where $j^{\,0}_{corr}$ and j_{corr} are the corrosion current densities for uninhibited and inhibited solutions, respectively.

3.3. *Impedance measurements*

3.3.1. *Effect of inhibitor concentration and temperature*

Figure 6 shows Nyquist plots recorded for copper in 3% NaCl solution at 25 °C without (Figure 6a) and with various concentrations of SO (Figure 6b) at the respective corrosion potentials. The influence of solution temperature on the impedance response of copper in (3% NaCl + 2.5×10^{-4} M SO) solution was studied at OCP; results are depicted in Figure 7. For the copper electrode without SO, a high frequency (HF) semicircle was observed followed by a straight line portion in the low-frequency (LF) region. The HF semicircle is attributed to the time constant of charge transfer and double-

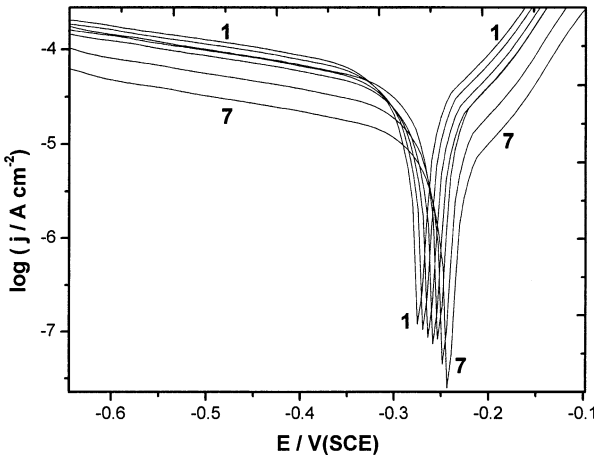

Fig. 4. Potentiodynamic anodic and cathodic polarization curves of a Cu electrode in 3% NaCl solution in the absence and presence of various concentrations of SO at a scan rate of 0.10 mV s^{-1} and at 25 °C. (1) Blank; (2) 2×10^{-5} M; (3) 5×10^{-5} M; (4) 8×10^{-5} M; (5) 10^{-4} M; (6) 2.5×10^{-4} M; (7) 5.0×10^{-4} M.

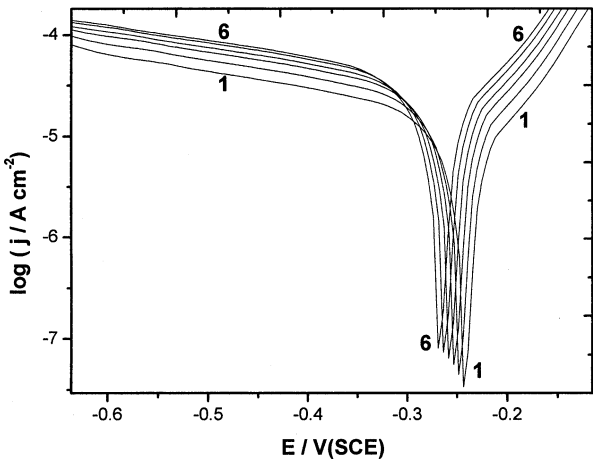

Fig. 5. Effect of temperature (15–65 °C) on the potentiodynamic anodic and cathodic polarization curves of a Cu electrode in (3% NaCl + 2.5×10^{-4} M SO) solution at a scan rate of 0.10 mV s^{-1}. (1) 15 °C; (2) 25 °C; (3) 35 °C; (4) 45 °C; (5) 55 °C; (6) 65 °C.

Table 2. The electrochemical parameters ($j_{corr.}$, $E_{corr.}$, b_c and b_a and R_p) associated with polarization measurements of Cu electrode in 3% NaCl solution containing 2.5×10^{-4} M SO at different temperatures

T/K	j_{corr} / μA cm^{-2}	E_{corr} / V(SCE)	b_a / V dec.$^{-1}$	b_c / V dec.$^{-1}$	R_p / kΩ
288	0.24	−0.2421	0.077	−0.128	8.86
298	0.32	−0.2473	0.076	−0.127	6.58
308	0.40	−0.2552	0.078	−0.127	5.32
318	0.46	−0.2572	0.076	−0.128	4.53
328	0.53	−0.2650	0.078	−0.127	4.00
338	0.58	−0.2677	0.076	−0.126	3.62

layer capacitance [3, 4]. This semicircle makes an angle approaching 65° with the real axis and its intersection gives a value of 1.75Ω cm^2 for the resistance of the solution (R_s) enclosed between the working electrode and the counter electrode. The intercept of the HF charge transfer semicircle with the real axis gives the charge transfer resistance (R_{ct}) value [26]. The LF linear

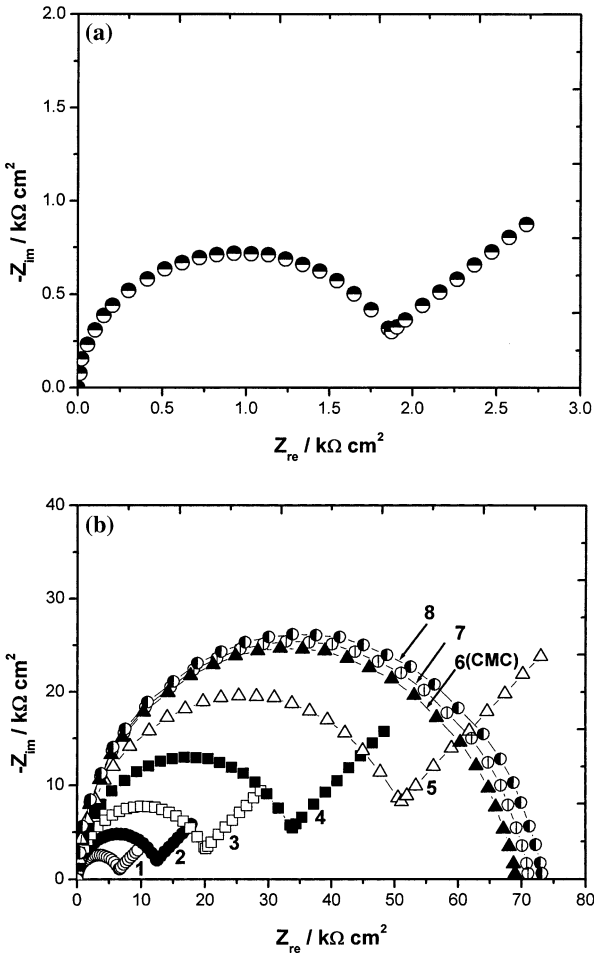

Fig. 6. (a) impedance response of a Cu electrode in 3% NaCl solution at the OCP and at 25 °C. (b) impedance response of a Cu electrode in 3% NaCl solution containing various concentrations of SO solution at the respective corrosion potentials and at 25 °C. (1) 2.5×10^{-4} M; (2) 5×10^{-4} M; (3) 7.5×10^{-4} M; (4) 1.0×10^{-3} M; (5) 1.25×10^{-3} M; (6) 1.5×10^{-3} M (CMC); (7) 1.75×10^{-3} M; (8) 2×10^{-3} M.

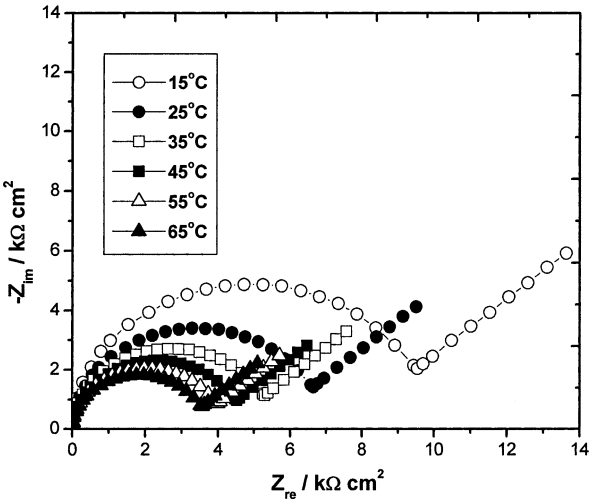

Fig. 7. Influence of solution temperature (15–65 °C) on the impedance responses of a Cu electrode in 3% NaCl solution containing 2.50×10^{-4} M SO at the respective corrosion potentials.

portion is generally believed to be a Warburg type impedance related to the diffusion of soluble copper species ($CuCl_2^-$) from electrode surface to bulk solution [3, 4]. To obtain the double layer capacitance (C_{dl}), the frequency (f_{max}) at which the imaginary component of the impedance is maximal was found and used in equation 8:

$$C_{dl} = 1/2\pi f_{max} R_{ct} \tag{8}$$

The inhibition efficiency was evaluated by R_{ct} and C_{dl} values of the impedance. The more densely packed the inhibitor surface film, the larger the diameter of the semicircle, which results in higher R_{ct} and lower C_{dl} values. Results of the present work showed that the R_{ct} values increase with increasing SO concentration, while the C_{dl} values tend to decrease (see the relation in Figure 8). The decrease in C_{dl} values is due to the adsorption of SO on the metal surface [27]. The reverse changes were produced by increasing temperature, as shown in Figure 7. The R_{ct} values were used to calculate the IE% of SO at different concentrations and temperatures (see Figure 2), using equation 9.

$$\text{IE\%} = 100 \times [(R_{ct} - R_{ct}^0)/R_{ct}] \tag{9}$$

where R_{ct}^0 and R_{ct} are the charge transfer resistances for uninhibited and inhibited solutions, respectively. It is apparent that the inhibition efficiency increases with increasing inhibitor concentration and tends to attain a maximum value when the concentration reaches values close to its critical micellar concentration. Moreover, the inhibition efficiency decreases with increasing temperature, confirming the suggestion that physical adsorption occurs. It is worth noting from Figure 2 that the inhibition efficiencies obtained from impedance measurements are comparable and run parallel with those obtained from weight loss and potentiodynamic polarization methods.

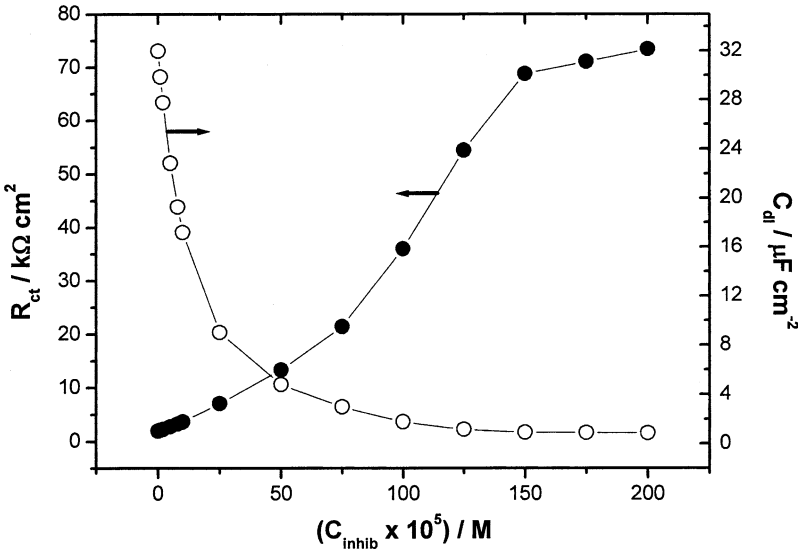

Fig. 8. Variation of R_{ct} and C_{dl} with SO concentration at the OCP and at 25 °C.

The large semicircle observed from high to low frequencies in the presence of inhibitor indicates that the charge-transfer resistance became dominant in the corrosion process due to the formation of an SO film on the copper surface. However, the Warburg impedance in the LF region is still visible at SO concentrations below CMC (as shown in Figure 6b; curves 1–5), indicating that the corrosion process is controlled by mixed charge-transfer and diffusion in solution. On the other hand, at SO concentrations equal to and higher than CMC, Warburg impedance at the LF region disappears (see curves 6–8 in Figure 6b). This disappearance of the Warburg impedance could be due to the formation of a protective film of the inhibitor on the copper surface (more details are shown in section 3.6).

The impedance data were interpreted according to two suitable equivalent circuits depicted in Figure 9. The first equivalent circuit (Figure 9a) was used to stimulate the EIS data displaying a Warburg impedance, while the second one (Figure 9b) was used to fit the EIS data displaying a capacitive loop. In these two circuits, R_s is the solution resistance, R_{ct} is the charge transfer resistance, C_{dl} is the double-layer capacitance, and Z_d represents the diffusion impedance appearing in the LF region.

One constant phase element (CPE) is substituted for the capacitive element to give a more accurate fit [28], as the obtained capacitive loop is a depressed semi-circle rather than regular one. The CPE is a special element whose immittance value is a function of the angular frequency (ω), and whose phase is independent of the frequency. Its admittance and impedance are, respectively, expressed as:

$$Y_{CPE} = Y_0(j\omega)^n \tag{10}$$

and

$$Z_{CPE} = (1/Y_0)[(j\omega)^n]^{-1} \tag{11}$$

where Y_0 is the magnitude of the CPE, j is the imaginary number ($j^2 = -1$), α is the phase angle of the CPE and $n = \alpha/(\pi/2)$. The factor n is an adjustable parameter that usually lies between 0.50 and 1.0 [29]. The CPE describes an ideal capacitor when $n = 1$. Values of α are usually related to the roughness of the electrode surface. The smaller value of α, the higher the surface roughness [5, 28]. The measured complex plane impedance plot is similar to that calculated by the equivalent circuit models. The points in Figure 6 and the following impedance plots represent the experimental data, while the solid curves represent the best fits.

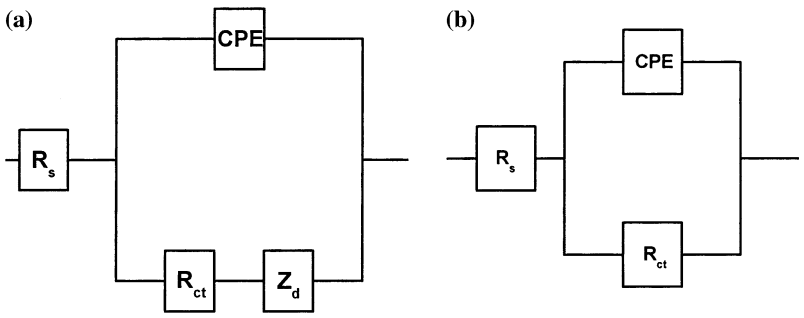

Fig. 9. (a) Equivalent circuit used to fit the EIS data for copper displaying a Warburg impedance. (b) Equivalent circuit used to fit the EIS data for copper displaying a capacitive loop.

3.3.2. *Effect of immersion time*

Electrochemical impedance spectroscopy is a useful technique for long time tests, because they do not significantly disturb the system and it is possible to follow it overtime [30]. Immersion time experiments in the present work were carried out in (3% NaCl + 2.5×10^{-4} M SO) solution for 720 min and Nyquist plots were recorded every 10 min during the first hour, and then every 60 min afterward. The results obtained (not shown here) showed that the immersion time has a significant influence on the size and shape of the impedance spectra, and therefore the inhibition efficiency of SO. The capacitive loop was found to increase in size with increase in immersion time, reaching a maximum in 50 min, and remained fairly constant afterward. The Warburg impedance was still visible during the initial 50 min and then disappeared.

More details are shown in Figure 10, which represents the variation for R_{ct} and C_{dl} with immersion time. It is clear that the R_{ct} values increased sharply from 7.09 to 100 kΩ cm^2 during the initial 50 min and remained fairly constant afterward. At the same time, the capacitance values were reduced drastically from 9.03 to 0.64 μF cm^{-2} after 50 min. These results demonstrate that the formation of the inhibitor surface film, and therefore the inhibitor adsorption, on the fresh copper surface was relatively fast and completed within 50 min.

3.3.3. *Determination of the PZC of copper in NaCl solutions*

Adsorption of surfactants on a corroding metal depends mainly on the charge of the metal surface, the charge or the dipole moment of surfactants, and the adsorption of other ionic species if it is electrostatic in nature [16]. The potential of zero charge (PZC) plays a very important role in the electrostatic adsorption process. The PZC of copper in 0.01 M Na_2SO_4 solution is −0.214 V(SCE) according to Bockris and Reddy [31], while it is −0.14 V (SCE) in 0.50 M H_2SO_4 solution [14]. The PZC of copper in NaCl solutions has not been found. The ac impedance study was used to evaluate the potential of zero charge (PZC) [28, 32]. A plot of C_{dl} values recorded for copper in 3% NaCl solution at each applied potential is shown in Figure 11, which is a parabola with a minimum capacitance at about −0.49 V(SCE). This value can be called the PZC of copper in 3% NaCl solution, which is more negative than the corrosion potential [−0.28 V(SCE)]. This means that the copper surface is positively charged at the corrosion potential.

3.4. *Mode of adsorption of SO on the copper surface*

The inhibitive action of SO in NaCl solution results from physical (electrostatic) adsorption of the negatively charged oleate ions to the positively charged copper surface, forming a barrier on the copper surface. In the early stages of adsorption (low surface coverage), i.e., at low SO concentrations and at low immersion times, the adsorption of the hydrocarbon chain (due to the presence of "–CH=CH–" group) and the electrostatic adsorption of the oleate ions on the copper surface take place simultaneously. This model suggests that the adsorbed oleate ions cover a large area, thereby inhibiting copper corrosion effectively.

When the immersion time and SO concentration increase, more oleate ions adsorb electrostatically on the copper surface. In this case, the physi-sorption of the hydrocarbon chain may be ignored. A hemimicelle barrier composed of oleate ions will form over the whole surface due to the interaction between hydrocarbon chains via van der Waals forces. The barrier becomes more compact and protective with adsorption of more

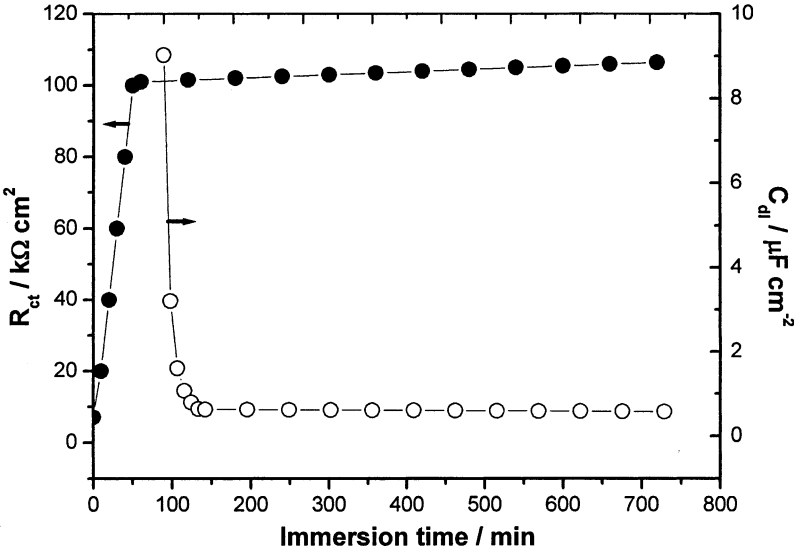

Fig. 10. Dependence of R_{ct} and C_{dl} on on the immersion time for cu electrode in 3% NaCl solution containing 2.50×10^{-4} M SO solution at the OCP and at 25 °C.

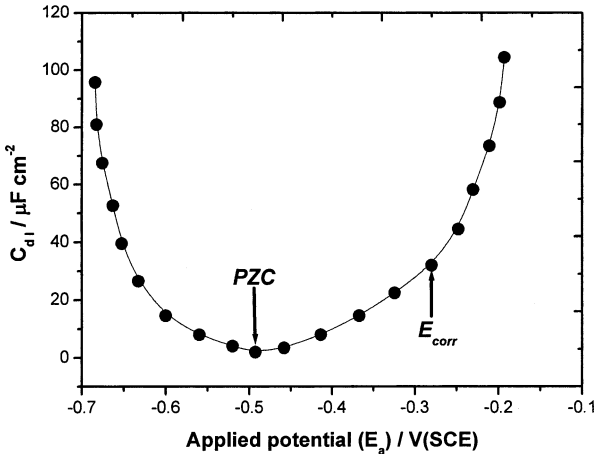

Fig. 11. Relationship between C_{dl} values and the applied potential for a copper electrode in 3% NaCl solution at 25 °C.

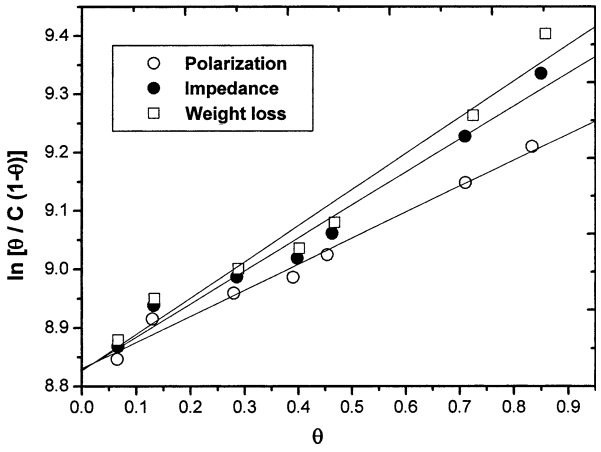

Fig. 12. Curve fitting of weight loss, polarization and impedance data obtained for a Cu electrode in 3% NaCl solution containing 2.50×10^{-4} M SO to Frumkin isotherm at 25 °C.

oleate ions on the surface. In this way, the inhibition efficiency of SO increases with increase in immersion time and concentration.

3.5. *Adsorption isotherms*

Adsorption isotherms are very important in determining the mechanism of organo-electrochemical reactions [32]. The most frequently used isotherms are Langmiur, Frumkin, Hill de Boer, Parsons, Temkin, Flory-Huggins and Dahar-Flory-Huggins and Bockris-Swinkel [33–41]. All these isotherms are of the general form:

$$f(\theta, x)\exp(-2a\theta) = KC \tag{12}$$

where f (θ, x) is the configurational factor which depends upon the physical model and the assumptions underlying the derivation of the isotherm, θ the surface coverage (θ = I.E/100), C the inhibitor concentration in the bulk of solution, "a" the lateral interaction term describing the molecular interactions in the adsorption layer and the heterogeneity of the surface (this is a measure for the steepness of the adsorption isotherm). K the adsorption-desorption equilibrium constant. In this study, the Frumkin adsorption isotherm (equation 13) was found to fit the experimental data obtained from the three techniques (see Figure 12).

$$KC = [\theta/(1-\theta)]\exp(-2a\theta) \tag{13}$$

The isotherm parameters (K and a) obtained from the Frumkin adsorption isotherm are shown in Table 3. The values of K decrease with increase in temperature. Large values of K mean better inhibition efficiency, i.e., strong electrical interaction between the double layer existing at the phase boundary and the adsorbing inhibitor molecules. Small values of K, however, compromise such interactions between adsorbing inhibitor molecules and the metal surface so that the inhibitor molecules are easily removable by the solvent molecules from the surface. These results confirm the suggestion that this inhibitor is physically adsorbed and the strength of adsorption decreases with temperature. Small and positive values of "a" indicate the existence of weak lateral forces of attraction between adsorbate molecules in the adsorption layer [42].

The free energies of adsorption (ΔG^0_{ads}) were calculated from the equation [42]:

$$K = (1/55.5)\exp(-\Delta G^0_{ads}/\mathrm{RT}) \tag{14}$$

where 55.5 is the concentration of water in the solution in mol l^{-1}, R is the universal gas constant and T is the thermodynamic temperature. It follows from the theory of adsorption from solutions [42] that:

$$(d\ \ln K/dT)_\theta = -\Delta H^0_{ads}/\mathrm{RT}^2 \tag{15}$$

where ΔH^0_{ads} is the isosteric enthalpy of adsorption. The integrated version of the Vant Hoff equation:

Table 3. Values of "K" and "a" for Cu in 3% NaCl solution containing 2.50×10^{-4} M SO obtained by applying Frumkin isotherm on the polarization and impedance data at different temperatures

T/K	K			a		
	Wt. loss	Polarization	Impedance	Wt loss	Polarization	Impedance
288	8111	7708	8103	0.27	0.21	0.26
298	6981	6836	6974	0.29	0.22	0.28
308	6317	6124	6311	0.29	0.24	0.29
318	5716	5597	5710	0.31	0.25	0.30
328	5276	5115	5271	0.32	0.26	0.31
338	4680	4582	4675	0.34	0.27	0.33

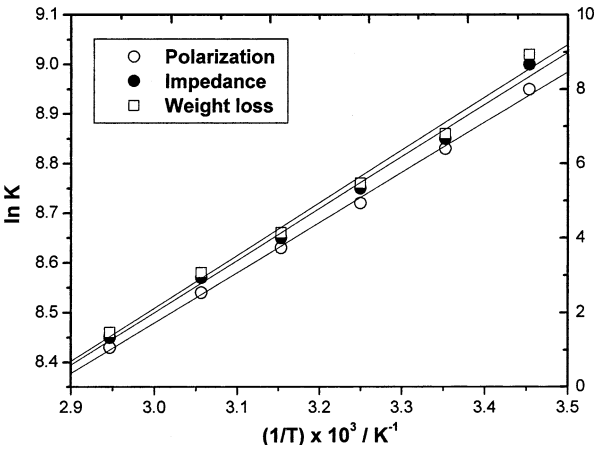

Fig. 13. Relation between log (binding constant) and $1/T$ for a Cu electrode in 3% NaCl solution containing 2.50×10^{-4} M SO to Frumkin isotherm at 25 °C obtained by applying Frumkin adsorption isotherm on weight loss, polarization and EIS data.

$$\ln K = -\Delta H^0_{ads}/\mathrm{RT} + \text{constant} \quad (16)$$

may be used to determine ΔH^0_{ads}. The slopes of the lines, shown in Figure 13, depict the linear relation between lnK and $(1/T)$ at a given surface coverage. These slopes multiplied by R give the values of ΔH^0_{ads}. The values of the entropy change of the inhibitor adsorption (ΔS^0_{ads}), was calculated from the equation:

$$\Delta G^0_{ads} = \Delta H^0 - T\Delta S^0_{ads} \quad (17)$$

Table 4 presents the thermodynamic parameters of adsorption ($\Delta G^0_{ads}, \Delta H^0_{ads}$ and ΔS^0_{ads}) obtained from the three methods by applying the Frumkin adsorption isotherm for Cu in 3% NaCl containing various surfactant concentrations at OCP and at 25 °C.

The negativity of the free energies of adsorption (ΔG^0_{ads}), shown in Table 4, means that the adsorption process is spontaneous. The absolute value of the adsorption enthalpy, $|\Delta H^0_{ads}|$, increases with increase in surface coverage due to the attractive interaction between the adsorbed molecules indicating the validity of the Frumkin model [43]. The origin of the attractive forces is most probably the dipole–dipole interaction occurring between the neighbouring adsorbed molecules [44]. The negativity of the enthalpy means that heat is released from the adsorption process. Generally, an exothermic adsorption process signifies either physi- or chemi-sorption, while an endothermic process is attributable unequivocally to chemi-sorption [45]. In an exothermic process, physi-sorption is distinguished from chemi-sorption by considering the absolute value of adsorption enthalpy. Typically, the enthalpy of a physi-sorption process is lower than 41.86 kJ mol^{-1}, while that of a chemi-sorption process approaches 100 kJ mol^{-1} [46]. In the present work, the absolute values of enthalpy are relatively low approaching those typical of physi-sorption. Table 4 clearly shows that the values of ΔS^0_{ads} decrease with increasing inhibitor concentration.

It is worth noting from the data of Table 4 that the absolute values of ΔH^0_{ads} and ΔG^0_{ads} increase with increasing inhibitor concentration, and tend to reach maximum values at inhibitor concentrations close to the CMC. In addition, ΔS^0_{ads} decreases with increasing inhibitor concentration and goes to negative values at concentrations close to the CMC. These results suggest that the highest inhibition efficiency is obtained when the SO concentration reaches a value close to its CMC. The trend of ΔS^0_{ads} with inhibitor concentration may be due to replacement of water molecules from the surface during adsorption of inhibitor molecules, resulting in a decrease in disordering [47].

3.6. *EDX and SEM examinations of the electrode surface*

EDX survey spectra were used to determine which elements were present on the copper surface before and after exposure to the inhibitor solution. Figure 14 presents spectra for copper samples exposed for 30, 60 and 120 min in 3% NaCl with and without added

Table 4. The thermodynamic parameters of adsorption process obtained from the polarization and impedance data by applying Frumkin isotherm for Cu in 3% NaCl solution containing various concentrations of the surfactant at OCP and at 25 °C

$C_{inhib} \times 10^5$/M	Wt. loss			Polarization			Impedance		
	ΔH^0_{ads}/ kJ mol^{-1}	ΔG^0_{ads}/ kJ mol^{-1}	ΔS^0_{ads}/ J $mol^{-1}K^{-1}$	ΔH^0_{ads}/ kJ mol^{-1}	ΔG^0_{ads}/ kJ mol^{-1}	ΔS^0_{ads}/ J $mol^{-1}K^{-1}$	ΔH^0_{ads}/ kJ mol^{-1}	ΔG^0_{ads}/ kJ mol^{-1}	ΔS^0_{ads}/ J $mol^{-1}K^{-1}$
1	−4.86	−25.12	67.99	−4.90	−25.14	67.93	−4.84	−25.10	68.00
2	−6.51	−26.43	66.85	−6.45	−26.41	66.99	−6.40	−26.38	67.05
5	−7.80	−27.20	65.11	−7.84	−27.30	65.31	−7.78	−27.00	64.50
8	−11.00	−29.00	60.41	−11.12	−29.12	60.41	−10.95	−28.96	60.44
10	−14.90	−31.00	54.03	−15.02	−31.09	53.93	−14.78	−30.93	54.20
25	−16.66	−32.50	53.16	−16.71	−32.61	53.36	−16.63	−32.45	53.09
50	−23.34	−34.38	37.05	−23.50	−34.42	36.65	−23.25	−34.35	37.25
75	−30.68	−35.99	17.82	−30.74	−36.05	17.82	−30.62	−35.96	17.92
100	−36.60	−37.10	1.68	−36.65	−37.17	1.75	−35.92	−36.50	1.94
125	−37.55	−37.25	−1.01	−37.62	−37.31	−1.04	−37.51	−37.21	−1.00
150 (CMC)	−37.73	−37.40	−1.11	−37.80	−37.44	−1.21	−37.69	−37.37	−1.08
175	−37.97	−37.42	−2.75	−38.05	−37.34	−2.38	−37.91	−37.43	−2.85
200	−38.35	−37.44	−3.09	−38.41	−37.50	−3.05	−38.30	−37.46	−3.02

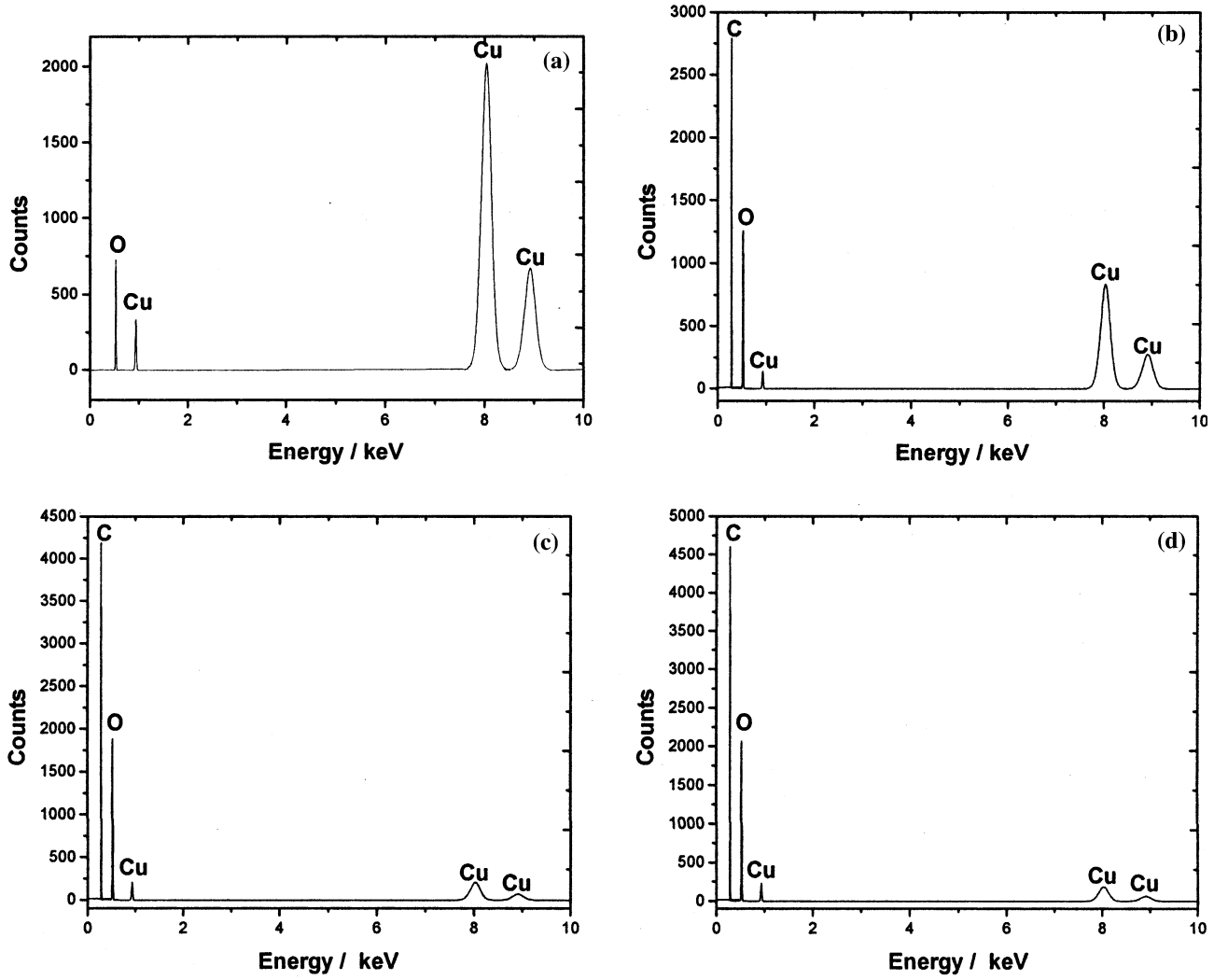

Fig. 14. EDX spectra of copper specimens (a) after 30 min of immersion in 3% NaCl solution. (b) after 30 min of immersion in (3% NaCl + 2×10^{-3} M SO) solution. (c) after 60 min of immersion in (3% NaCl + 2×10^{-3} M SO) solution. (d) after 120 min of immersion in (3% NaCl + 2×10^{-3} M SO) solution.

inhibitor (2.0×10^{-3} M). In uninhibited NaCl solutions, the EDX spectra (Figure 14a) confirm the existence of cuprite crystals (Cu_2O), as indicated by the Cu and O signals. However, in inhibited NaCl solutions (Figure 14b-d), the EDX spectra showed an additional line characteristic of the existence of C (due to the carbon atoms of SO). In addition, the O signal is significantly enhanced due to the two oxygen atoms present in the carboxylate group of SO. These data show that a carbonaceous material containing oxygen atoms has covered the electrode surface. This layer is undoubtedly due to the inhibitor, because the carbon signal and the high contribution of the oxygen signal are not present on the copper surface exposed to uninhibited NaCl solutions (see Figure 14a). In addition, the intensity of the carbon and oxygen signals increase with immersion time (see Figure 14b–d), since more oleate ions will electrostatically adsorb on the fresh copper surface.

The spectra of Figure 14b–d show that the Cu peaks are considerably suppressed relative to the samples prepared in 3% NaCl solution, and this suppression increases with immersion time. The suppression of the Cu lines occurs because of the overlying inhibitor film. These results confirm those from polarization measurements which suggest that a surface film inhibited the growth of copper oxide, and hence retarded the reduction of dissolved oxygen in the NaCl solution. The inhibitor surface film acts as a barrier to the diffusion of oxygen molecules from solution to copper substrate [48], which may increase the overpotential of cathodic reduction of dissolved oxygen, as shown in Figure 1. This surface film also increases the charge transfer resistance of the anodic dissolution of copper (Figure 6b), slowing down the corrosion rate. This may explain the disappearance of the Warburg impedance at high immersion times and concentrations.

The formation of a protective surface film of inhibitor on the electrode surface was further confirmed by SEM observations after 30, 60 and 120 min immersion in uninhibited and inhibited NaCl solutions, as shown in Figure 15. The SEM micrograph shows the initial growth of cuprite crystals in 3% NaCl solution

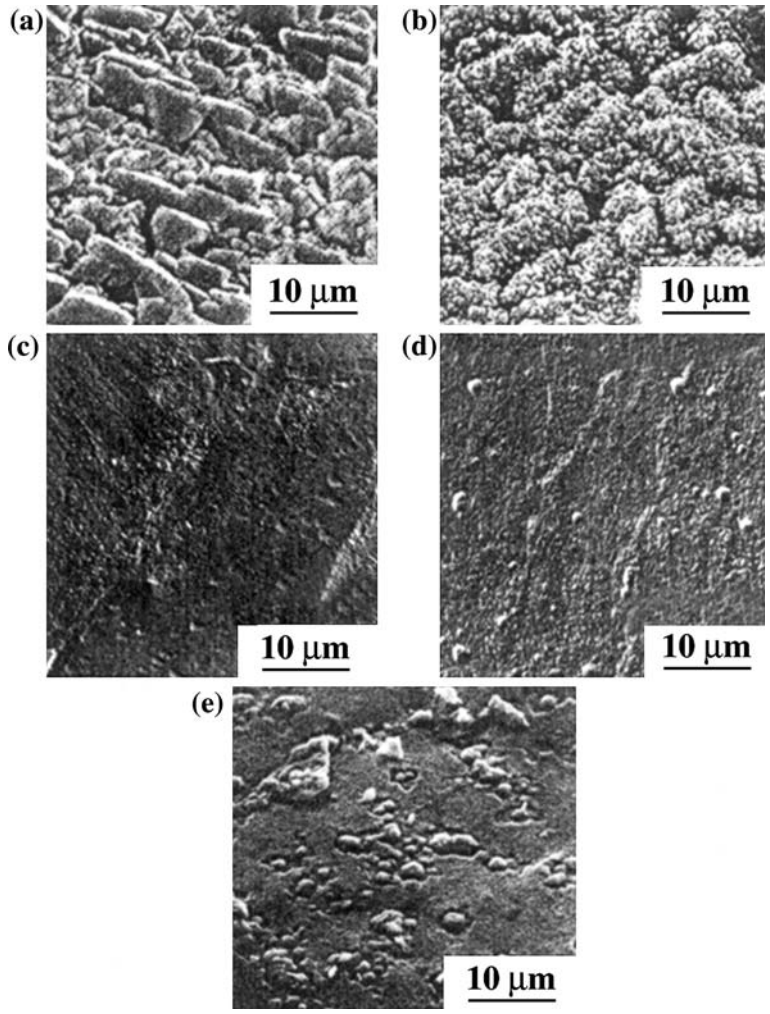

Fig. 15. SEM images of copper specimens (a) after 30 min of immersion in 3% NaCl solution. (b) after 60 min of immersion in 3% NaCl solution. (c) after 30 min of immersion in (3% NaCl + 2×10^{-3} M SO) solution. (d) after 60 min of immersion in (3% NaCl + 2×10^{-3} M SO) solution. (e) after 120 min of immersion in (3% NaCl + 2×10^{-3} M SO) solution.

(Figure 15a), followed by the successive formation of a surface layer of very small crystals (Figure 15b). In inhibited solution, the copper surface is free of corrosion products (Figure 15c) and only after 60 and 120 min does some roughness appear (see Figure 15d and e).

4. Conclusion

Weight loss, polarization, AC impedance, SEM and EDX were used to study the corrosion inhibition of copper in aerated stagnant 3% NaCl solution at the corrosion potential using sodium oleate (SO) as an anionic surfactant inhibitor. The principle conclusions are

(i) The corrosion of copper in NaCl solutions is significantly reduced upon the addition of SO.
(ii) Inhibition efficiency increases with increasing SO concentration and immersion time, while it decreases with temperature. Maximum inhibition efficiencies were observed at concentrations around the critical micellar concentration.
(iii) SEM and EDX observations of the electrode surface showed that a surface film of inhibitor is formed on the electrode surface. This film retarded the reduction of dissolved oxygen and inhibited the growth of copper oxide in the NaCl solution (mixed-type inhibitor).
(iv) Physisorption is proposed as the mechanism for corrosion inhibition.
(v) The inhibition efficiencies obtained from polarization data are comparable with those obtained from impedance measurements.
(vi) The data obtained from the three techniques fit the Frumkin adsorption isotherm well.

References

1. A.L. Bacarella and J.C. Griess, *J. Electrochem. Soc.* **120** (1973) 459.
2. W.H. Smyrl, *in* B.E. Conway, E. Yeager and R.E. White, (Eds), 'Comprehensive Treatise of Electrochemistry', Vol. 4, J.O'M. Bockris, (Plenum Press, New York, 1981), pp. 97–149.

3. O.E. Barcia, O.R. Mattos, N. Pebere and B. Tribollet, *J. Electrochem. Soc.* **140** (1993) 2825.
4. C. Deslouis, B. Tribollet, G. Mengoli and M.M. Musiani, *J. Appl. Electrochem.* **18** (1988) 374.
5. A.V. Benedetti, P.T.A. Sumodjo, K. Nobe, P.L. Cabot and W.G. Proud, *Electrochim. Acta* **40** (1995) 2657.
6. G. Zhou, H. Shao and B.H. Loo, aa. *J. Electroanal. Chem.* **421** (1997) 129.
7. F.K. Crundwell, *Electrochim. Acta* **37** (1992) 2101.
8. H.P. Lee and K. Nobe, *J. Electrochem. Soc.* **133** (1986) 2035.
9. C. Fiaud, 8th Eur. Symp. on Corrosion Inhibitors. *Ann. Univ. Ferrara* **2** (1995) 929.
10. R. Gasparac, C.R. Martin and E. Stupnisek-Lisac, *J. Electrochem. Soc.* **147** (2000) 548.
11. E. Stupnisek-Lisac, A. Gazivoda and M. Madzarac, *Electrochim. Acta* **47** (2002) 4189.
12. H. Otmacic and E. Stupnisek-Lisac, *Electrochim. Acta* **48** (2003) 985.
13. F. Mansfeld and Y. Wang, *in* 'Corrosion 95', NACE, Paper No. 41, 1995.
14. H. Ma, S. Chen, S. Zhao, X. Liu, D. Liu and D. Li, *J. Electrochem. Soc.* **148** (2001) B482.
15. G. Trabanelli *in* F. Mansfeld (Ed.), 'Corrosion Mechanisms', (Marcel Dekkar, Inc., New York, 1987), p. 119.
16. H. Luo, Y.C. Guan and K.N. Han, *Corrosion* **54** (1998) 619.
17. C.A. Miller and S. Qutubuddin, *in* H.-F, Eike and C.D. Parfitt (Eds), Interfacial Phenomena in polar Media, 'Surfactant Science Series', Vol. 21, (Marcel Dekker, Inc., New York 1987), p. 166.
18. H. Ma, S. Chen, B. Yin, S. Zhao and X. Liu, *Corros. Sci.* **45** (2003) 867.
19. S.S. Abd El-Rehim, H.H. Hassan and M.A. Amin, *Mat. Chem. & Phys.* **70** (2001) 64.
20. S.S. Abd El-Rehim, H.H. Hassan and M.A. Amin, *Mat. Chem. & Phys.* **78** (2002) 337.
21. S.S. Abd El-Rehim, H.H. Hassan and M.A. Amin, *Corros. Sci.* **46** (2004) 5–25.
22. N.S. Tarasova, M.A. Khachaturyan and L.A. Nikolaev, *Russ. J. Phys. Chem.* **58** (1984) 628.
23. B.A. Boukamp, *Equivalent Circuit* (Princeton Applied Research Corporation, Princeton, N J, 1990).
24. T. Zhao and G. Mu, *Corros. Sci.* **41** (1999) 1937.
25. M.J. Rosen, *in* 'Surfactants and Interfacial Phenomena', (Wiley, New York, 1978), pp. 1–301.
26. H.H. Hassan, *Appl. Surf. Sci.* **174** (2001) 201.
27. F. Bentiss, M. Lagrence, M. Traisnel and J.C. Hornez, *Corros. Sci.* **41** (1999) 789.
28. X. Wu, H. Ma, S. Chen, Z. Xu and A. Sui, *J. Electrochem. Soc.* **146** (1999) 1847.
29. (a) B.A. Boukamamp, *Solid State Ionics*, **20** (1980) 31; (b) International Report CT 89/214/128, University of Twente, Eindhoven, The Netherlands (1989).
30. G. Moretti, F. Guidi and G. Grion, *Corros. Sci.* **46** (2003) 387.
31. J.O'M. Bockris, A.K.N. Reddy, *in* J.O'M. Bockris, B.E. Conway, E. Yeager and R.E. White (Eds), 'Modern Electrochemistry', Vol. 2, (Plenum Press, New York, 1970), p. 708.
32. B.B. Damaskin, O.A. Petrii and B. Batraktov, *Adsorption of Organic Compounds on Electrodes* (Plenum Press, New York, 1971).
33. I. Langmuir, *J. Am. Chem. Soc.* **39** (1917) 1848.
34. R. Alberty and R. Silbey, *Physical Chemistry*, 2nd ed., (Wiley, New York, 1997), pp. 845.
35. J.O'M. Bockris and S.U.M. Khan, *Surface Electrochemistry: A Molecular Level Approach* (Plenum Press, New York, 1993).
36. J.W. Schapinik, M. Oudeman, K.W. Leu and J.N. Helle, *Trans. Farad. Soc.* **56** (1960) 415.
37. A.N. Frumkin, *Z. Phys. Chem.* **116** (1925) 466.
38. O. Ikeda, H. Jimbo and H. Tamura, *J. Electroanal. Chem.* **137** (1982) 127.
39. J. Hill de Boer, 'The Dynamical Character of Adsorption', 2nd edn., (Clarendon Press, Oxford, UK, 1986).
40. H. Dhar, B. Conway and K. Joshi, *Electrochim. Acta* **18** (1973) 789.
41. E. Kamis, I. Mellucci, R.M. Lantanision and E.S.H. El-Ashry, *Corrosion* **47** (1991) 677.
42. D. Do, 'Adsorption Analysis: Equilibria and Kinetics', (Imperial College Press, 1998), pp. 10–60.
43. B. Conway, *Principles of Electrode Processes* (The Ronald Press Company, New York, 1965), pp. 78–85.
44. S. Martinez, *Mater. Chem. & Phys.* **77** (2003) 97.
45. W. Durnie, R. De Marco, B. Kinsella and A. Jefferson, *J. Electrochem. Soc.* **146** (1999) 1751.
46. S. Martinez and I. Stern, *Appl. Surf. Sci.* **199** (2002) 83.
47. M.J. Lampinen and M. Fomino, *J. Electrochem. Soc.* **140** (1993) 3537.
48. M. Ishibashi, M. Itoh, H. Nishihara and K. Aramaki, *Electrochim. Acta* **41** (1996) 241.